PHYSICAL REVIEW D **96,** 084012 (2017)

Novel phase transition in charged dilaton black holes

Amin Dehyadegari,[1] Ahmad Sheykhi,[1,2,*] and Afshin Montakhab[1,†]

[1]*Physics Department and Biruni Observatory, Shiraz University, Shiraz 71454, Iran*

[2]*Research Institute for Astronomy and Astrophysics of Maragha (RIAAM), P.O. Box 55134-441, Maragha, Iran*

(Received 19 July 2017; published 5 October 2017)

We disclose a novel phase transition in black hole physics by investigating thermodynamics of charged dilaton black holes in an extended phase space where the charge of the black hole is regarded as a fixed quantity. Along with the usual critical (second-order) as well as the first-order phase transitions in charged black holes, we find that a finite jump in Gibbs free energy is generated by the dilaton-electromagnetic coupling constant α for a certain range of pressure. This novel behavior indicates a small/large black hole *zeroth-order* phase transition the thermodynamic response function of black hole diverges, e.g., isothermal compressibility. Such zeroth-order transition separates the usual critical point and the standard first-order transition curve. We show that increasing the dilaton parameter (α) increases the zeroth-order portion of the transition curve. Additionally, we find that the second-order (critical) phase transition exponents are unaffected by the dilaton parameter; however, the condition of positive critical temperature puts an upper bound on the dilaton parameter ($\alpha < 1$).

DOI: 10.1103/PhysRevD.96.084012

I. INTRODUCTION

Since the discovery of black hole thermodynamics in the 1970s by Bekenstein [1] and Hawking [2], physicists have been speculating that there should be some kind of thermodynamic phase transition in this gravitational system. Hawking and Page were the first to discover a first-order phase transition of thermal radiation, large black holes in the background of Schwarzschild anti–de-Sitter (AdS) spacetime [3]. Later, by considering charged black holes, a phase transition was shown to occur between small-large black holes [4]. Such a phase transition has been associated to a liquid-gas transition such as the one occurring in the van der Waals system [5,6]. Recently, a phase transition of charged AdS black holes has attracted much attention. It was shown that thermodynamic properties of charged AdS black holes admit a first-order phase transition between large and small black holes, which is analogous to the van der Waals liquid-gas phase transition [7,8]. In this perspective, thermodynamic analyses are improved in an *extended phase space* in which the cosmological constant and its conjugate variable are considered as the thermodynamic pressure and volume, respectively. It has been demonstrated that the first law of black hole thermodynamics is consistent with the Smarr relation provided the mass of the black hole is identified as the enthalpy [9]. The phase transition and critical behavior of black holes in an extended phase space have been investigated in ample detail for various systems (see [10–18] and references therein) and, recently, in a more general framework in [19]. In all these works [7–19], the cosmological constant (pressure) is considered as a variable quantity, and the charge of the black holes is fixed. The holographic transition of dilaton gravity (e.g., superfluidity and superconductivity) has been studied in Ref. [20].

In another approach towards thermodynamic phase space of black holes, it was shown that one can think of variation of charge Q of a black hole and keep the cosmological constant as a fixed parameter. The motivation for this assumption comes from the fact that the charge of a black hole is a natural external variable which can vary [21]. In addition, the cosmological constant is related to the background of AdS geometry, and it is more natural to take it as a constant rather than a variable quantity [21]. This alternative view of such a phase space and more physically conventional description of the phase transition naturally leads to a meaningful response function and a more accurate analogy with the van der Waals fluid [21]. Indeed, in this perspective, the critical behavior occurs in the Q^2-Ψ plane, where $\Psi = 1/2r_+$ is the conjugate of Q^2 [21]. It was shown that a small-large black hole phase transition occurs with an associated critical point (T_c, Q_c^2, Ψ_c) with complete analogy with the van der Waals fluid system [21].

A discontinuity in the derivatives of Gibbs free energy with respect to temperature characterizes the type of phase transition that occurs in a thermodynamic system. A first-order phase transition has a discontinuity in the first derivative which is entropy, i.e., $(\partial G/\partial T) = S$, and a second-order (critical) phase transition has discontinuity (singularity) of $(\partial^2 G/\partial^2 T)$. Therefore, a lesser-known zeroth-order phase transition has a discontinuity in the Gibbs free energy itself, which was discovered in superfluidity and superconductivity [22]. The author of Ref. [22]

*asheykhi@shirazu.ac.ir
†montakhab@shirazu.ac.ir

also showed that a zeroth-order phase transition occurs in Bogolyubov's model of a weakly nonideal Bose gas. On the other hand, a novel reentrant phase transition has been recently observed to accompany the standard first-order phase transitions in black holes [23–27]. Motivated by the above novel phase transitions, we intend to present a study of small-large phase transitions in charged dilaton black holes. Therefore, we analyze the possible phase transitions in extended phase space for fixed charge where the spacetime geometry is described by Einstein-Maxwell-dilaton gravity [28]. We find that the presence of a dilaton parameter leads to a region of the phase diagram which allows for zeroth-, first-, and second-order phase transition where the zeroth order separates the first- and second-order transition along the transition curve. The extension of such a region becomes larger with increasing dilaton parameter.

This article is structured as follows: In Sec. II, we study the thermodynamics of $(d+1)$-dimensional charged dilaton black holes in the presence of Liouville-type dilaton potential. In Sec. III, we investigate the critical behavior of dilaton black holes. In Sec. IV, we study the equation of state of charged dilaton black holes. The last section is devoted to summary and conclusions.

II. BASIC THERMODYNAMICS OF THE CHARGED DILATON BLACK HOLE

The action of $(d+1)$-dimensional spacetime in Einstein-Maxwell theory with a scalar dilaton field (φ) reads [29]

$$\mathcal{I}=\frac{1}{16\pi}\int d^{d+1}x\sqrt{-g}\bigg(\mathcal{R}-\frac{4}{d-1}(\nabla\varphi)^2-\mathcal{V}(\varphi)-e^{-4\alpha\varphi/(d-1)}F_{\mu\nu}F^{\mu\nu}\bigg), \tag{1}$$

where $F_{\mu\nu}=\partial_{[\mu}A_{\nu]}$, A_ν is the vector potential, and α is the coupling parameter of the dilaton with Maxwell field. Hereon, $\mathcal{V}(\varphi)$ is the dilaton potential, which has the following form [28,29]

$$\mathcal{V}(\varphi)=2\Lambda e^{4\alpha\varphi/(d-1)}+\frac{(d-1)(d-2)\alpha^2}{b^2(\alpha^2-1)}e^{4\varphi/[(d-1)\alpha]}, \tag{2}$$

where b is a positive arbitrary constant. In the absence of the dialton field $(\alpha=0)$, the above potential reduces to $\mathcal{V}(\varphi)\to 2\Lambda$, and, thus, one may interpret Λ as the cosmological constant. The $(d+1)$-dimensional spherical symmetric metric is given by

$$ds^2=-f(r)dt^2+\frac{dr^2}{f(r)}+r^2R(r)^2d\Omega^2_{d-1}, \tag{3}$$

where $d\Omega^2_{d-1}$ is the line element of a unit $(d-1)$-sphere with the volume ω_{d-1}. Applying the ansatz $R(r)=e^{2\alpha\varphi/(d-1)}$, one can show that [28]

$$f(r)=\frac{2\Lambda(\alpha^2+1)^2r^{2(1-\gamma)}}{(d-1)(\alpha^2-d)b^{-2\gamma}}-\frac{(d-2)(\alpha^2+1)^2b^{-2\gamma}r^{2\gamma}}{(\alpha^2-1)(\alpha^2+d-2)}-\frac{m}{r^{(d-1)(1-\gamma)-1}}+\frac{2q^2(\alpha^2+1)^2r^{2(d-2)(\gamma-1)}}{(d-1)(\alpha^2+d-2)b^{2\gamma(d-2)}}, \tag{4}$$

$$\varphi(r)=\frac{(d-1)\alpha}{2(1+\alpha^2)}\ln\left(\frac{b}{r}\right),\qquad A_t=\frac{qb^{\gamma(3-d)}}{\Pi r^{\Pi}}, \tag{5}$$

where $\gamma=\alpha^2/(\alpha^2+1)$, $\Pi=(d-3)(1-\gamma)+1$, b is a positive arbitrary constant, and m and q, respectively, are related to the total mass and electric charge of the black hole [28]

$$M=\frac{b^{\gamma(d-1)}(d-1)\omega_{d-1}}{16\pi(\alpha^2+1)}m,\qquad Q=\frac{q\omega_{d-1}}{4\pi}. \tag{6}$$

Inasmuch as the event horizon is defined by the largest root of $f(r_+)=0$, one can write m in terms of r_+. The temperature, entropy, and electric potential of Einstein-Maxwell-dilaton black holes are obtained as [28]

$$T=-\frac{(d-2)(\alpha^2+1)b^{-2\gamma}}{4\pi(\alpha^2-1)}r_+^{2\gamma-1}-\frac{\Lambda(\alpha^2+1)b^{2\gamma}}{2\pi(d-1)}r_+^{1-2\gamma}-\frac{q^2(\alpha^2+1)b^{-2\gamma(d-2)}}{2\pi(d-1)}r_+^{(2d-3)(\gamma-1)-\gamma}, \tag{7}$$

$$S=\frac{b^{\gamma(d-1)}\omega_{d-1}}{4}r_+^{(d-1)(1-\gamma)},\qquad U=\frac{qb^{\gamma(3-d)}}{\Pi {r_+}^{\Pi}}. \tag{8}$$

In the Appendix, using Wald's formalism [9,30–33], we present a derivation of the first law of thermodynamics that includes a variation in the cosmological constant. We also show that the mass of the dilaton black hole is equivalent to enthalpy. Hence, the first law of thermodynamics and Smarr formula take the form,

$$dM=TdS+UdQ+VdP, \tag{9}$$

$$M=\frac{(d-1)(1-\gamma)}{\Pi}TS+UQ+\frac{(4\gamma-2)}{\Pi}VP, \tag{10}$$

in which P and V are the thermodynamic pressure and volume, respectively, given by

$$P=-\frac{(d+\alpha^2)b^{2\gamma}\Lambda}{8\pi(d-\alpha^2)r_+^{2\gamma}},\qquad V=\frac{(1+\alpha^2)\omega_{d-1}b^{(d-1)\gamma}}{d+\alpha^2}r_+^{(d+\alpha^2)/(1+\alpha^2)}. \tag{11}$$

In the absence of the dilaton $(\alpha=0)$, the above pressure becomes $P=-\Lambda/8\pi$, which is the pressure of the Reissner-Nordstrom-AdS (RN-AdS) black hole [8].

III. INSTABILITY AND PHASE TRANSITION IN THE DILATON BLACK HOLE

The sign of the response functions must be positive for local stability of a thermodynamic system [5]. Since we consider an extended phase space, it is important to study the behavior of the isothermal compressibility

$$\kappa_T = -\frac{1}{V}\frac{\partial V}{\partial P}\bigg|_T. \tag{12}$$

The negative sign of κ_T indicates local thermodynamic instability and, therefore, a phase transition in the system. To see the exact behavior of the thermodynamic system with regard to local instability, we need to calculate the Gibbs free energy $G = G(T, P)$, which is obtained as

$$G = M - TS = \left\{\frac{(d-2)(1+\alpha^2)b^{\gamma(n-3)}}{16\pi(\alpha^2+d-2)r_+^{(n-3)(\gamma-1)-1}} + \frac{P(\alpha^4-1)b^{\gamma(d-1)}}{(d-1)(d+\alpha^2)r_+^{d(\gamma-1)-\gamma}} + \frac{q^2(2d-3+\alpha^2)(\alpha^2+1)b^{\gamma(3-d)}}{8\pi(d-2+\alpha^2)(d-1)r_+^{(n-3)(1-\gamma)+1}}\right\}\omega_{n-1}. \tag{13}$$

Let us first consider the Gibbs free energy in the absence of the dilaton ($\alpha = 0$) depicted in Fig. 1 for $d = 3$. According to Fig. 1, the Gibbs energy is single valued and increases monotonically with the increasing pressure for $T > T_c$ and is locally stable ($\kappa_T > 0$) everywhere, as indicated by the solid blue line. However, for $T < T_c$, it becomes multivalued with negative κ_T shown by the dashed red line. Since the minimum value of G is chosen by the system at equilibrium, this indicates a first-order phase transition which occurs between the SBH and LBH where the slope of G is discontinuous at the transition point. At $T = T_c$, a second-order phase transition occurs between the SBH and LBH where G is single valued and continuous but is nonanalytic. The corresponding phase (P-T) diagram for RN-AdS black hole is illustrated in the inset of Fig. 1. The SBH is distinguished from the LBH by a transition line with a critical point at the end of the transition curve. Note that this transition curve looks analogous to the van der Waals P-T diagram. The qualitative behavior for higher-dimensional black holes is the same as $d = 3$.

Now, we turn to examine the effects of the dilaton field parameter ($\alpha \neq 0$) on the phase transition of black holes in extended phase space. For this purpose, we plot the Gibbs free energy as a function of pressure for $\alpha = 0.4$ and $d = 3$ in Fig. 2. One can see that for $T \geq T_c$, the behavior is similar to the previous case ($\alpha = 0$); namely, the Gibbs free energy is single valued and increases monotonically with increasing the pressure. Here, T_c is the critical point where a second-order phase transition occurs. In the range of temperature $T \leq T_{\rm f}$, where the loop is formed at $T = T_{\rm f}$, a *first-order* phase transition occurs similarly to the van der Waals fluid system. However, for the temperature range $T_{\rm f} < T < T_c$, an interesting phenomenon occurs where a finite jump in G leads to a zeroth-order phase transition. Such zeroth-order phase transition has previously been considered in the theory of superfluidity and superconductivity [22] and, more recently, has been reported as a part of reentrant phase transition in black holes [23–27].

To be more specific, let us consider the case of $T \approx 0.064 \in [T_{\rm f}, T_c]$ in Fig. 3. Decreasing the pressure of the system (despite its multivaluedness) follows a locally stable

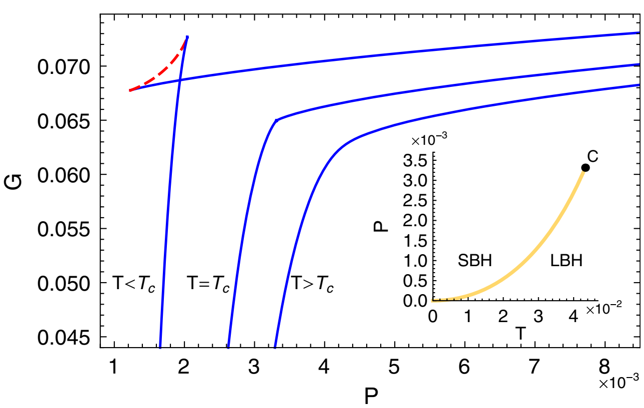

FIG. 1. Gibbs free energy as a function of pressure for $\alpha = 0$, $q = 1$, and $d = 3$ and different values of temperature. Below the critical temperature (T_c), it shows multivalued behavior indicating a first-order phase transition [small black hole (SBH)/large black hole (LBH)]. The positive (negative) sign of κ_T is identified by blue solid (dashed red) line. Note that various curves are shifted for clarity. The corresponding phase diagram (P-T) is shown in the inset.

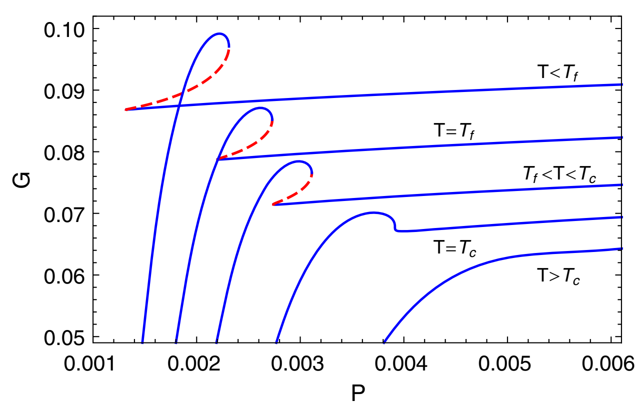

FIG. 2. Gibbs free energy as a function of pressure for different values of temperature and $\alpha = 0.4$, $b = 1$, $q = 1$, and $d = 3$. The positive (negative) sign of κ_T is identified by the blue solid (dashed red) line. For $T \leq T_c$, $G(P)$ develops nonanalytic behavior in different ways at $T = T_c$ for $T_{\rm f} < T < T_c$ and finally for $T < T_{\rm f}$. Note that various curves are shifted for clarity.

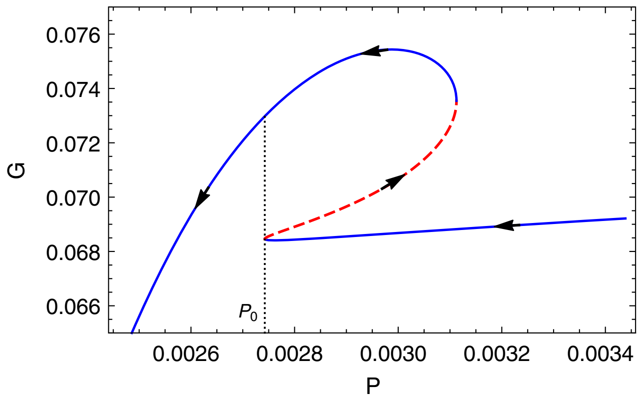

FIG. 3. A closeup of $T \approx 0.064 \in [T_f, T_c]$ in Fig. 2 displays a zeroth-order phase transition which is accompanied by a finite jump in G at $P_0 \approx 0.00274$. The positive (negative) sign of κ_T is identified by the blue solid (dashed red) line, and the arrows show the direction of the increasing r_+.

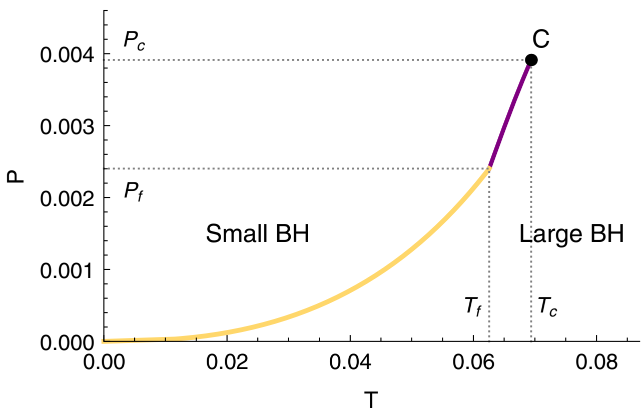

FIG. 4. Phase diagram corresponding to Fig. 2 for transition between the SBH and LBH. Three different transition are identified: first-order (gold curve), zeroth-order (purple curve), and a second-order critical point at (T_c, P_c).

regime ($\kappa_T > 0$) by choosing the lower G value. However, at $P = P_0$, a jump to a higher (stable) value of G is required, thus, leading to a discontinuous G and a zeroth-order phase transition. Note that this type of phase transitions is absent in normal liquid-gas transitions such as the van der Waals fluid.

The phase diagram of the charged dilaton black hole is shown in Fig. 4. A van der Waals–like first-order phase transition occurs for $(T, P) < (T_f, T_f)$. This is followed by zeroth-order phase transition curve with finite jump in G for the range $(T_f, T_f) < (T, P) < (T_c, T_c)$. Interestingly, the zeroth-order transition curve terminates at the critical point (T_c, T_c).

IV. EQUATION OF STATE

The equation of state $P = P(T, r_+)$ (for fixed q) can be obtained by using Eq. (7) as

$$P = \frac{(d+\alpha^2)(d-1)T}{4(d-\alpha^2)(1+\alpha^2)r_+} + \frac{(d-2)(d-1)(d+\alpha^2)b^{-2\gamma}}{16\pi(\alpha^2-1)(d-\alpha^2)r_+^{2-2\gamma}} + \frac{(d+\alpha^2)q^2b^{-2\gamma(d-2)}}{8\pi(d-\alpha^2)r_+^{1-(2d-3)(\gamma-1)+\gamma}}. \quad (14)$$

The $P - r_+$ isothermal diagrams for $\alpha = 0.4$ and $d = 3$ are shown in Fig. 5. The critical point is essentially an inflection point where ($\partial P/\partial r_+ = 0$ and $\partial^2 P/\partial r_+^2 = 0$) and can be obtained as [16]

$$P_c = \left[\frac{(d-1)(d-2)}{2(2d-3+\alpha^2)(d-1+\alpha^2)}\right]^{[\gamma-(2d-3)(\gamma-1)+1]/2\Pi} \times \left[\frac{(d+\alpha^2)(2d-3+\alpha^2)(d-2+\alpha^2)}{8\pi(1+\alpha^2)(d-\alpha^2)b^{2\gamma/\Pi}q^{2(1-\gamma)/\Pi}}\right], \quad (15)$$

$$T_c = \left[\frac{(d-1)}{2q^2(d-1+\alpha^2)}\right]^{(1-2\gamma)/2\Pi}\left(\frac{(\alpha^2+d-2)}{\pi(1-\alpha^2)b^{\gamma(n-1)/\Pi}}\right) \times \left[\frac{(2d-3+\alpha^2)}{(d-2)}\right]^{[(2d-3)(\gamma-1)-\gamma]/2\Pi}, \quad (16)$$

$$r_{+c} = \left[\frac{2q^2(d-1+\alpha^2)(2d-3+\alpha^2)b^{6\gamma-2d\gamma}}{(d-2)(d-1)}\right]^{1/2\Pi}. \quad (17)$$

According to Eq. (16), the critical temperature has positive values if the dilaton parameter is restricted to $\alpha < 1$. One can calculate the critical exponents $\alpha' = 0$, $\beta' = 1/2$, $\delta' = 3$, and $\gamma' = 1$ associated with the second-order transition, which are mean-field values such as the van der Waals fluid system [16].

For $T < T_c$, we observe local instability ($\kappa_T < 0$) and negative pressure in some range of quantities for the system. Such an unphysical behavior is remedied by choosing the globally stable Gibbs free energy as illustrated in Fig. 2. For $T < T_f$, where a first-order phase transition occurs, a globally unphysical part is replaced by the isobar line for which $G_{\mathrm{SBH}} = G_{\mathrm{LBH}}$. Following the behavior of Gibbs free energy, we observe that the modified isobar line for the zeroth-order phase transition starts at the point of local minimum of isotherm for range $T_f < T < T_c$. One can see from Fig. 5 that κ_T diverges ($\partial P/\partial r_+ = 0$) in the case of zeroth-order phase transition. Similarly, one can plot the entropy (S) versus temperature (T) as well and will subsequently see that the heat capacity at the constant pressure diverges in the zeroth-order phase transition.

Figure 6 shows a SBH/LBH phase diagram for various values of the dilaton parameter α. As is seen from the figure, increasing α from zero (RN-AdS BH) will lead to the creation and elongation of the zeroth-order phase transition as the critical point moves higher, and the first-order transition curve (purple) bends lower and further in the P-T space. Finally, it is worth mentioning that similar

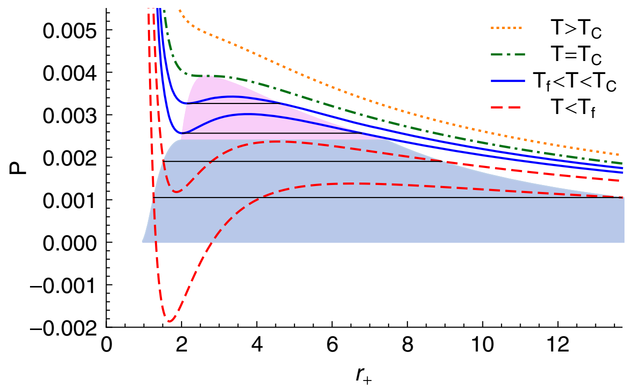

FIG. 5. $P - r_+$ diagram of charged dilaton black holes for various temperatures and $\alpha = 0.4$, $b = 1$, $q = 1$, and $d = 3$. The regions of zeroth- and first-order phase transition are characterized by different colors. The isobars (black thin line) remedy the unphysical locally and globally unstable regimes; see Fig. 2.

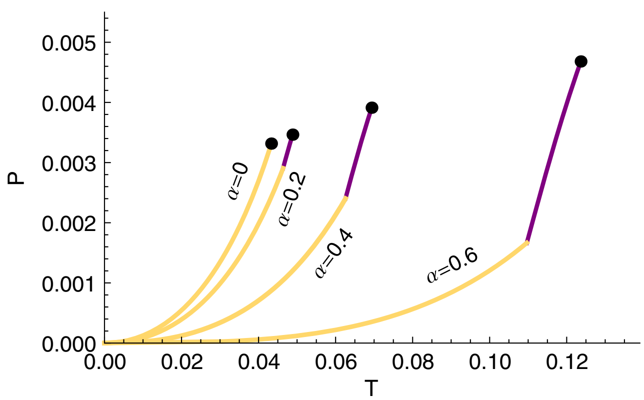

FIG. 6. SBH/LBH phase diagram for various values of the dilaton parameter α and $b = 1$, $q = 1$, and $d = 3$. Increasing α leads to a larger portion of the transition curve belonging to the zeroth-order phase transition. The critical points are highlighted by a black solid circle.

qualitative behavior for the higher-dimensional ($d > 3$) charged dilaton black holes can be observed.

V. SUMMARY

In this paper, we have investigated the thermodynamic phase behavior of charged dilaton black holes in the presence of Liouville-type dilaton potentials. Because of the presence of the dilaton field, these solutions are neither asymptotically flat nor (A)dS [28]. We have disclosed the effects of the dilaton field on the phase transition properties of charged black holes in an extended phase space. In addition to the usual small/large black hole transition (first and second order) [7,8], we have observed a *zeroth-order* phase transition between a small and large black hole in which isothermal compressibility and heat capacity at the constant pressure diverge. In addition, the Gibbs free energy has a finite jump at the point where a *zeroth-order* phase transition occurs. We have also obtained that a zeroth-order phase transition emerges in a longer portion of the transition line by increasing a coupling constant of the dilaton field. It is worth noting that a coupling constant is restricted to $\alpha < 1$, for which the critical temperature is positive. Finally, we have shown a set of critical exponents which are the same with the van der Waals fluid system.

ACKNOWLEDGMENTS

The support of Shiraz University research council is kindly acknowledged. The work of A. S. has been supported financially by Research Institute for Astronomy & Astrophysics of Maragha, Iran.

APPENDIX A: THE FIRST LAW OF THERMODYNAMICS FOR DILATON BLACK HOLE WITH THE VARIATION OF COSMOLOGICAL CONSTANT

To prove a version of the first law of thermodynamics with varying cosmological constant Λ in a dilaton black hole, we utilize a Hamiltonian approach by applying the Noether current formalism of Wald which was obtained earlier in [30,31,33]. For simplicity of calculation, we do not consider the charge of the black hole and also set $d = 3$. The variation of the Hamiltonian that generates translation along a Killing vector ξ is given as [30,32]

$$\delta H[\xi] = \int_{\mathcal{C}} d\Sigma_a \frac{\omega^a}{\sqrt{-g}}, \tag{A1}$$

where $\mathcal{C}$ is a Cauchy surface and $d\Sigma_a = n_a \sqrt{h} d^3 y$. Here, h is the determinant of a three-dimensional hypersurface with the normal field n_a. In Eq. (A1), ω^a for Einstein gravity coupled to a scalar (dilaton) field is given as [33]

$$\omega^a = -\delta(\sqrt{-g} J^a) + \frac{\sqrt{-g}}{8\pi}\left[\nabla_b(\xi^{[a}\delta v^{b]}) - \frac{\partial \mathcal{V}(\varphi)}{2\partial\Lambda}\xi^a \delta\Lambda\right], \tag{A2}$$

in which

$$\delta v^a = \nabla_b \delta g^{ab} - \nabla^a \delta g^b_b - 4\delta\varphi\nabla^a\varphi. \tag{A3}$$

In the absence of the dilaton ($\varphi = 0$), Eqs. (A2) and (A3) reduce to expressions calculated in the AdS black hole [32]. The Noether current in Eq. (A2) is $J^a = \nabla_b J^{ab} = \frac{1}{8\pi}\nabla_b(\nabla^{[a}\xi^{b]})$, where J^{ab} is the antisymmetric Noether potential [30,33]. By using Eqs. (A2) and (A3) and applying Stokes's theorem, one can write Eq. (A1) as

$$\delta H[\xi] = -\frac{1}{2}\delta\int_{\mathcal{H}} d\Sigma_{ab}J^{ab} + \frac{1}{2}\delta\int_{\partial\mathcal{C}_\infty} d\Sigma_{ab}J^{ab} - \frac{1}{16\pi} \times \int_{\partial\mathcal{C}_\infty} d\Sigma_{ab}\xi^{[a}\delta v^{b]} - \frac{\delta\Lambda}{16\pi}\int_{\mathcal{C}} d\Sigma_a \frac{\partial\mathcal{V}(\varphi)}{\partial\Lambda}\xi^a, \tag{A4}$$

where $\mathcal{H}$ is the bifurcation surface, and $\partial\mathcal{C}_\infty$ is a boundary of $\mathcal{C}$ at infinity. Note that the timelike Killing vector vanishing on the bifurcation surface does not contribute to Eq. (A4). In this situation, $\delta H[\xi] = 0$ does not mean $H[\xi]$ is zero. Then one can recognize the first term on the right-hand side of Eq. (A4) as $-\kappa\delta S/2\pi$ after the horizon Killing field is normalized to unit surface gravity κ [30]. The second and third terms are identified as δM where the Killing vector approaches an asymptotic time translation [30]. Now, we interpret the last term of Eq. (A4) as $-V\delta P$, which can be written as

$$V\delta P = \delta\Lambda/16\pi\int_{\mathcal{H}} n_a\xi^a\sqrt{h}d^3y\frac{\partial\mathcal{V}(\varphi)}{\partial\Lambda}, \tag{A5}$$

where the divergence term in the above equation is omitted by adding a suitable counterterm [32]. Inserting Eq. (2) into the above expression and taking into account Eq. (5), we can rewrite Eq. (A5) as

$$V\delta P = b^{2\gamma}\delta\Lambda/8\pi\int_{\mathcal{H}}\frac{n_a\xi^a\sqrt{h}d^3y}{r^{2\gamma}}. \tag{A6}$$

Hence, according to the metric (3) and thermodynamic pressure Eq. (11), one can easily calculate the thermodynamic volume in Einstein dilaton gravity as

$$V = \frac{4\pi(1+\alpha^2)b^{2\gamma}}{3+\alpha^2}r_+^{(3+\alpha^2)/(1+\alpha^2)}. \tag{A7}$$

Also, one can find that from Eq. (A4), the first law of the dilaton black hole with varying cosmological constant takes the form

$$\delta M = T\delta S + V\delta P, \tag{A8}$$

in which $T = \kappa/2\pi$. In this regard, the mass of the dilaton black hole is interpreted as the enthalpy rather than the internal energy.

[1] J. D. Bekenstein, Phys. Rev. D **7**, 2333 (1973); **9**, 3292 (1974).
[2] S. W. Hawking, Commun. Math. Phys. **43**, 199 (1975); Phys. Rev. D **13**, 191 (1976).
[3] S. Hawking and D. N. Page, Commun. Math. Phys. **87**, 577 (1983).
[4] A. Chamblin, R. Emparan, C. Johnson, and R. Myers, Phys. Rev. D **60**, 064018 (1999); **60**, 104026 (1999).
[5] H. B. Callen; *Thermodynamics and an Introduction to Thermostatistics*, 2nd ed. (John Wiley & Sons, New York, 1985).
[6] D. C. Johnston, arXiv:1402.1205.
[7] B. P. Dolan, Classical Quantum Gravity **28**, 125020 (2011); **28**, 235017 (2011).
[8] D. Kubiznak and R. B. Maan, J. High Energy Phys. 07 (2012) 033.
[9] D. Kastor, S. Ray, and J. Traschen, Classical Quantum Gravity **26**, 195011 (2009).
[10] B. P. Dolan, Phys. Rev. D **84**, 127503 (2011); Fortschr. Phys. **62**, 892 (2014).
[11] M. Cvetic, G. W. Gibbons, D. Kubiznak, and C. N. Pope, Phys. Rev. D **84**, 024037 (2011).
[12] M. Urana, A. Tomimatsu, and H. Saida, Classical Quantum Gravity **26**, 105010 (2009).
[13] S.-W. Wei and Y.-X. Liu, Phys. Rev. D **87**, 044014 (2013).
[14] De. Zou, Y. i. Liu, and B. Wang, Phys. Rev. D **90**, 044063 (2014).
[15] S. H. Hendi and M. H. Vahidinia, Phys. Rev. D **88**, 084045 (2013); S. H. Hendi, S. Panahiyan, and B. Eslam Panah, Int. J. Mod. Phys. D **25**, 1650010 (2016).
[16] M. H. Dehghani, S. Kamrani, and A. Sheykhi, Phys. Rev. D **90**, 104020 (2014).
[17] M. H. Dehghani, A. Sheykhi, and Z. Dayyani, Phys. Rev. D **93**, 024022 (2016).
[18] Z. Dayyani, A. Sheykhi, and M. H. Dehghani, Phys. Rev. D **95**, 084004 (2017).
[19] B. R. Majhi and S. Samanta, Phys. Lett. B **773**, 203 (2017).
[20] A. Salvio, J. High Energy Phys. 09 (2012) 134; 03, (2013) 136.
[21] A. Dehyadegari, A. Sheykhi, and A. Montakhab, Phys. Lett. B **768**, 235 (2017).
[22] V. P. Maslov, Mathematical notes of the Academy of Sciences of the USSR **76**, 697 (2004).
[23] S. Gunasekaran, R. B. Mann, and D. Kubiznak, J. High Energy Phys. 11 (2012) 110.
[24] N. Altamirano, D. Kubiznak, and R. B. Mann, Phys. Rev. D **88**, 101502 (2013); N. Altamirano, D. Kubiznak, R. B. Mann, and Z. Sherkatghanad, Classical Quantum Gravity **31**, 042001 (2014); S. W. Wei, P. Cheng, and Y. X. Liu, Phys. Rev. D **93**, 084015 (2016).
[25] A. M. Frassino, D. Kubiznak, R. B. Mann, and F. Simovic, J. High Energy Phys. 09 (2014) 080; De. Zou, Y. Lio, and B. Wang, Phys. Rev. D **90**, 044063 (2014); R. A. Hennigar, W. G. Brenna, and R. B. Mann, J. High Energy Phys. 07 (2015) 077;

M. B. J. Poshteh, B. Mirza, and Z. Sherkatghanad, Phys. Rev. D **88**, 024005 (2013).
[26] R. A. Hennigar and R. B. Mann, Entropy **17**, 8056 (2015).
[27] N. Altamirano, D. Kubiznak, R. B. Mann, and Z. Sherkatghanad, Galaxies **2**, 89 (2014); D. Kubiznak and F. Simovic, Classical Quantum Gravity **33**, 245001 (2016).
[28] A. Sheykhi, Phys. Rev. D **76**, 124025 (2007).
[29] K. C. K. Chan, J. H. Horne, and R. B. Mann, Nucl. Phys. **B447**, 441 (1995).
[30] R. M. Wald, Phys. Rev. D **48**, R3427 (1993).
[31] J. Couch, W. Fischler, and P. H. Nguyen, J. High Energy Phys. 03 (2017) 119.
[32] K. Bhattacharya and B. R. Majhi, Phys. Rev. D **95**, 104024 (2017).
[33] T. Faulkner, M. Guica, T. Hartman, R. C. Myers, and M. Van Raamsdonk, J. High Energy Phys. 03 (2013) 51.